ACI STRUCTURAL JOURNAL TECHNICAL PAPER

Title No. 111-S116

Database of Shear Tests for Non-Slender Reinforced Concrete Beams without Stirrups

by Karl-Heinz Reineck and Leonardo Todisco

A database is presented with shear tests on non-slender beams without stirrups subjected to point loads with shear span to effective depth ratios (a/d) < 2.4. From the 338 collected shear tests, 222 tests remained for the evaluations after several selection criteria were applied. The tests were compared with the left part of the shear valley by Kani and did not confirm the strength increase up to the flexural strength in the range from a/d = 2.4 to approximately 1.0. The test results were compared to the strut-and-tie model according to ACI 318-11. The model overestimated the test results. The reduction factor for the strength of the unreinforced struts should be reduced to $\beta_s = 0.42$ instead of 0.60 for a strut without reinforcement, such as the inclined strut transferring the load to the support for a point load near an end support.

Keywords: beams; database; reinforced concrete; shear reinforcement; shear slenderness; shear strength; shear tests; strut-and-tie models.

INTRODUCTION

The new extended databases for shear tests on reinforced concrete beams without stirrups subjected to point loads were presented by Reineck et al. (2006, 2010, 2012) in which 1365 shear test on beams without stirrups were collected. The data were sorted into the two control files: vuct-RC-DK-sl for slender beams with shear span ratios $(a/d) \geq 2.4$; and vuct-RC-DK-24 for non-slender beams with $a/d < 2.4$. The former are further investigated by Reineck et al. (2013), whereas the latter is further presented in this paper.

The shear slenderness is defined for a beam with a point load by the distance a between the axis of the point load and the support axis, as shown in Fig. 1 along with the simplest possible strut-and-tie model. The angle θ shall not be taken less than 25 degrees according to A.2.5 of Appendix A of ACI 318-11. This leads to the following condition for the maximum distance a_{max}

$$a_{max}/z = \cot\theta = \cot 25 \text{ deg} = 2.144 \quad (1a)$$

Assuming $z = 0.9 \cdot d$ for the inner lever arm, this gives

$$a_{max} = 1.93d \quad (1b)$$

This value is only slightly less than the above defined limit $a/d = 2.40$ assumed for the division between slender and non-slender beams. Therefore, these databases for non-slender beams presented herein enable the comparison of the test results with the capacity of the simple model shown in Fig. 1, which complies with A.2.5 of Appendix A of ACI 318-11. Such comparisons were performed by Todisco (2011). In addition, comparisons are also possible for empirical relationships of the shear capacity proposed for the influence of the shear slenderness on the shear capacity.

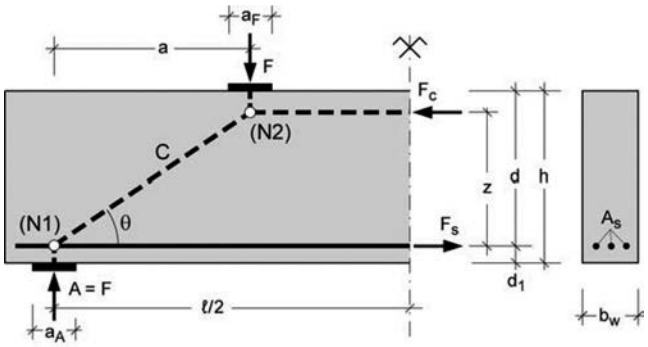

Fig. 1—Simple strut-and-tie model for non-slender beams.

RESEARCH SIGNIFICANCE

Shear design provisions in codes for members without shear reinforcement have mostly been empirically derived and consequently reliable databases are of vital importance for comparing such provisions with test results. The database presented herein deals with non-slender reinforced concrete (RC) beams without stirrups subjected to point loads with $a/d < 2.4$ for the shear slenderness. The tests can be compared with the well-known shear valley by Kani. The simple strut-and-tie model and the strength values can be checked, which are proposed in A.2.5 of Appendix A of ACI 318-11.

DATABASE WITH SHEAR TESTS ON NON-SLENDER RC BEAMS WITHOUT STIRRUPS SUBJECTED TO POINT LOADS

Introduction

The new extended database for tests on RC beams without stirrups subjected to point loads was presented by Reineck et al. (2013) and it includes 1365 collected test beams. The data were sorted into the two control files: vuct-RC-DK-sl for slender beams with $a/d \geq 2.4$; and vuct-RC-DK-24 for 331 non-slender beams with $a/d < 2.4$. The first is further dealt with by Reineck et al. (2013), whereas the latter is presented in the following. In addition to the previously 331 tests, seven more tests could be added recently so that

ACI Structural Journal, V. 111, No. 6, November-December 2014.

Table 1—Results of the evaluation of the tests in respect of the individual criteria koni

Individual criteria	Condition for criterion	Tests satisfying criterion		Violating criterion
		No.	Percent of 338	No.
kon1	$f_{1c} > 12$ MPa (1.74 ksi)	328	99.1	10
kon2	$f_{1c} < 100$ MPa (14.5 ksi)	337	99.7	1
kon3	$b_w \geq 50$ mm (2 in.)	338	100.0	0
kon31	$50 \leq b_w < 100$ mm (4 in.)	30	8.9	—
kon4	$h > 70$ mm (2.755 in.)	338	100.0	0
kon41	$70 < h < 150$ mm (5.9 in.)	7	2.1	—
kon7	$\xi_{test} = x/d \leq 0.5$	332	98.2	6
kon8	$\beta_{flex} = \mu_u/\mu_{flex} < 1.00$	239	70.7	99
kon81	$1.00 \leq \beta_{flex} \leq 1.10$	37	10.9	—
kon82	$\beta_{flex} \leq 1.10$	276	81.6	62
kon10	$f_r = r$: ribbed	309	91.4	29
kon11	$\beta_{lb} = l_{b,req}/l_{b,prov} < 1.0$	295	87.3	43
kon15	No “oft”	298	88.2	40

the control file vuct-RC-DK-24 now contains 338 tests for checking the different criteria.

Control of data

Check of anchorage at end support—The check of the anchorage of the longitudinal bars at the end support in this database has to consider that the beams are non-slender, so that for loads near to the support, the force in the bars at the end support cannot be calculated according to the truss analogy as was done for slender beams. For a load in a distance $a \leq z$, it is assumed that the simple strut-and-tie model in Fig. 1 fully applies, and so the force in the longitudinal reinforcement to be anchored at the end support is

$$F_{sA} = F \cdot a/z \tag{2}$$

In the region $z < a < 2.4 \cdot z$, a portion of the load can be directly transferred to the end support and the rest is transferred by the truss. As a simplification, it is assumed that the anchorage check for slender beams remains valid in this range.

Results of checks for different criteria—The database vuct-RC-DK_24 for non-slender beams comprises 338 shear tests on beams without stirrups subjected to point loads in a distance $a/d < 2.4$. These beams are examined by means of some control criteria and the remaining beams are transferred to the data evaluation file. Individual criteria were defined and checked for:

- koni = 0 not fulfilled; not transferred to evaluation file;
- koni = 1 fulfilled; transferred to evaluation file.

The abbreviation “kon” is a German acronym for control criterion and “i” is a running number. The criteria are explained in detail by Reineck et al. (2003, 2006, 2010, 2012) as well as in Table 1, where the results of the checks for the individual criteria are listed.

Table 2—Subsequent application ofindividual selection criteria for KONA0 and for evaluation databases KONA24b and KONA24d, respectively

Selection criterion	Combination of individual criteria	Added criterion	Remain of 338	Difference
KONA0a	kon1 · kon3 · kon4 · kon7	—	329	9
KONA0b	KONA0a · kon10	$f_r = r$: ribbed	303	26
KONA0	KONA0b · kon15	No ”oft”	270	33
KONA24a	KONA0 · kon8	$\beta_{flex} = \mu_u/\mu_{flex} < 1.00$	215	55
KONA24b	KONA24a · kon11	$\beta_{lb} = l_{b,req}/l_{b,prov} < 1.0$	201	14
KONA24c	KONA0 · kon82	$\beta_{flex} \leq 1.00$	238	32
KONA24d	KONA24c · kon11	$\beta_{lb} = l_{b,req}/l_{b,prov} < 1.0$	222	16

The first criteria from kon1 to kon7 are fulfilled by almost all tests. The criterion kon31 applies to 30 tests that would not be considered in evaluations if the minimum web width depth is increased from 50 to 100 mm (2 to 4 in.). Likewise, criterion kon41 that 7 tests would not be considered in evaluations if the minimum depth is increased from 70 to 150 mm (2.76 to 5.9 in.).

The strict criterion kon8 ($\beta_{flex} < 1.0$) for the check whether a flexural failure had occurred was only fulfilled by 239 (71%) of the 338 tests. The additional criterion kon81 accounts for some of the conservativeness of the standard flexural strength calculations, so that additionally 37 tests (11%) could be regarded as to have passed the flexure check (refer to kon82).

The criterion kon11 for the check of the end anchorage of the longitudinal bars was only fulfilled by 87% of the tests. The criterion kon15 “oft” means no “other failure type” and is a check against failure modes not reported as shear failures; this applied to 40 tests (12%).

Selection of tests for the evaluation—To be transferred to the evaluation file, several criteria must be fulfilled simultaneously for a beam, and this means:

KONAi = 0 no transfer to evaluation file;

KONAi = 1 transfer to evaluation file.

All of the tests considered for the evaluation have to fulfill the following set of criteria:

$$\text{KONA0} = \text{kon1} \cdot \text{kon3} \cdot \text{kon4} \cdot \text{kon7} \cdot \text{kon10} \cdot \text{kon15}$$

Table 2 shows the subsequent application of the individual selection criteria until the dataset KONA0 was found in which 270 beams remained. Finally, in order to be transferred to the evaluation file, the criteria kon8 for the flexural check and kon11 for the anchorage check must be fulfilled leading to the datasets KONA24b with 201 tests (refer to Table 2). If instead of kon8, the criterion kon82 is accepted, then 21 more tests remain in the dataset KONA24d with 222 tests.

Presentation of evaluation database for non-slender RC beams without stirrups subjected to point loads—In the following, 222 tests of the dataset KON24d are presented by plotting the number of tests in selected ranges versus the main test parameters.

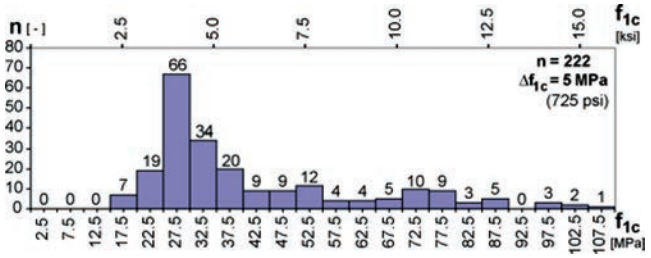

Fig. 2—Number of beams plotted versus uniaxial concrete compressive strength f_{1c} *for database vuct-RC-A24d.*

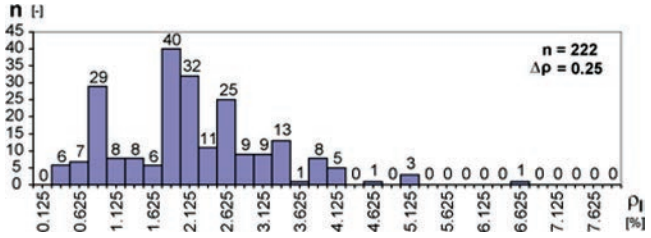

Fig. 3—Number of beams versus geometrical reinforcement ratio ρ_l *(=* ρ_w *in ACI) for database vuct-RC-A24d.*

In Fig. 2, the number n of beams is plotted versus the uniaxial concrete compressive strength f_{1c} (= $0.95f_{c,cyl}$) subdivided in class intervals of Δf = 5 MPa (725 psi). The majority of tests were carried out for a uniaxial compressive strength of concrete between 20 and 35 MPa (2.9 and 5.0 ksi), which made up 119 tests (54%). Relatively few (42) tests (19%) were performed on beams with HSC with f_{1c} > 60 MPa (8.7 ksi).

The geometrical reinforcement ratio $\rho_l = A_s/(b_w \cdot d)$ (= ρ_w in ACI 318-11) is often considered in design formulas, and in Fig. 3, the number of beams is plotted versus ρ_l subdivided in class intervals of $\Delta\rho_l$ = 0.25%. Many beams were highly reinforced and 118 tests (approximately 53%) contained a reinforcement ratio of ρ_l > 2.0%. Only 42 tests (19%) had low reinforcement ratios of ρ_l < 1.0%, and from these, only six tests (3%) had values ρ_l < 0.50%, representing the range most common in practice.

In Fig. 4, the number of the beams is plotted versus the effective depth d subdivided in class intervals of Δd = 100 mm. The peak of 80 tests (36%) is in the range between d = 200 and 300 mm (8 and 12 in.), and the vast majority of tests—that is, 190 (86%)—had effective depths of d < 500 mm (approximately 20 in.). Only one test had a high effective depth of d > 1000 mm (40 in.).

COMPARISON WITH KANI'S TESTS

The evaluation database vuct-RC-24d contains 222 tests on non-slender beams with a shear span ratio a/d < 2.4. In this range, the ultimate shear force increases with decreasing a/d, as can be seen in the nondimensional Fig. 5, where the nondimensional shear force υ_u is defined as

$$\upsilon_u = V_u/(b_w \cdot z \cdot f_{1c}) \quad (3)$$

where z is the inner lever arm; b_w is the web width; and f_{1c} is uniaxial compressive strength = $0.95f_c'$.

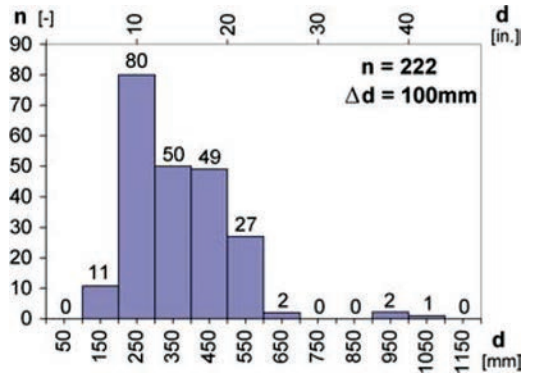

Fig. 4—Number of beams plotted versus effective depth d *for database vuct-RC-A24d. (Note: 1 mm = 0.0394 in.)*

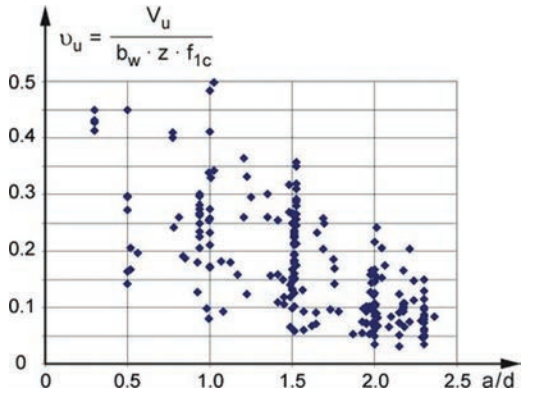

Fig. 5—Nondimensional shear force υ_u *versus shear span ratio* a/d *for the 222 tests of evaluation database vuct-RC-A24d.*

Figure 5 shows an increase of the shear capacity with decreasing a/d. However, this also applies to the shear force for the flexural capacity. Therefore, Kani (1964, 1966) related the shear capacity to the flexural capacity and proposed his well-known shear valley, shown in Fig. 6 for a test series. This ratio (named β_{flex} herein) is defined as

$$\beta_{flex} = M_u/M_{flex} = V_u/V_{flex} \quad (4)$$

The maximum moment and the shear force of the beam $V = F$ shown in Fig. 1 are related by

$$M = V \cdot a \quad (5a)$$

Because the moment for a flexural failure is known for given materials, the corresponding shear force can be calculated from Eq. (5a) as

$$V_{flex} = M_{flex}/a \quad (5b)$$

The test results by Kani (1966) for β_{flex} are plotted versus a/d in Fig. 6 for beams with a longitudinal reinforcement ratio of ρ_l = 1.88% and with three concrete strengths. The longitudinal reinforcement ratio ρ_l (= ρ in ACI 318-11) is defined as

$$\rho_l = A_s/b \cdot d \quad (6)$$

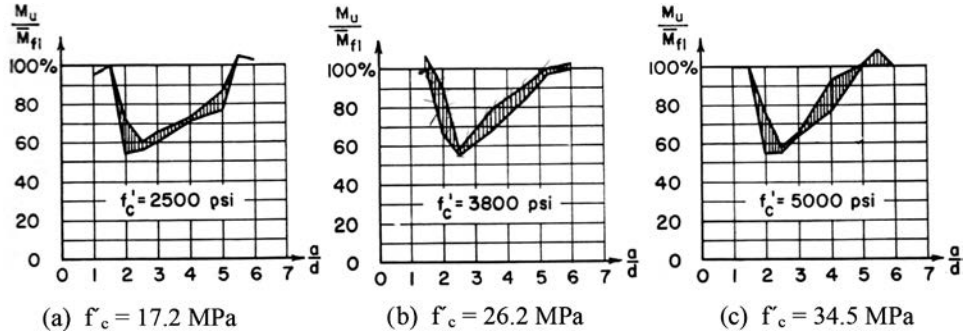

Fig. 6—Test results M_u/M_{flex} *(=* β_{flex}*) versus* a/d *shown in Fig. 6 of Kani (1966) for beams with* ρ_l *= 1.88% and different concrete strengths.*

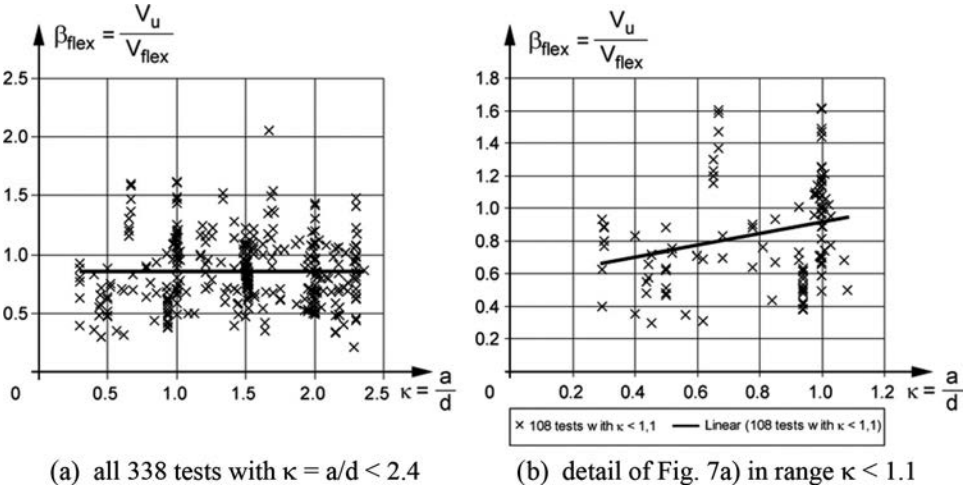

Fig. 7—Ratio $\beta_{flex} = V_u/V_{flex}$ *plotted versus* κ = a/d *for all 338 tests of database.*

where A_s is the area of longitudinal reinforcement; b is the width of the compression zone; and d is the effective depth.

The left parts of the Fig. 6(a), (b), and (c) show a drastic decrease of shear capacity with increasing a/d, from approximately $a/d = 1$ up to approximately $a/d = 2.5$, which is almost the range of the database presented herein. Kani (1964, 1966) explained this behavior by an arching action.

The database represents tests with $a/d < 2.4$, which can be compared with the left parts of the valleys shown in Fig. 6. The values β_{flex} for all 338 tests in the database are plotted in Fig. 7 versus the a/d, and these also contain the tests with $\beta_{flex} > 1.1$. The mean is $\beta_{flex} = 0.86$ (refer to Fig. 7(a)) and the trend line is almost horizontal and does not exhibit a decrease for β_{flex} with increasing a/d, as exhibited in Fig. 6 in the left part of the shear valley. The tests in the range $\kappa < 1.1$ (refer to Fig. 7(b)) even exhibit a decrease of β_{flex} with decreasing $\kappa = a/d$, and this clearly contradicts the left parts of the shear valley in Fig. 6, whereby there are no tests by Kani with $\kappa < 0.98$ in the database. This statement is not diminished by the scatter of the tests with a relatively high coefficient of variation $v = 38\%$ in the range $\kappa = a/d < 1.1$. The trend is clear and it should be noted that all tests with shear-span ratios $\kappa = a/d \le 0.6$ in Fig. 7(b) fall well below $\beta_{flex} = 1.0$ until down to $\beta_{flex} = 0.3$.

To directly compare the results of the specific test series in Fig. 7 by Kani with other tests of the database, the other tests had to be selected with values of ρ_l and f_c' as near as possible to the values for the test series by Kani. Thereby allowances were given of approximately ± 12% for deviations from $\rho_l = 1.88\%$ and from the values for f_c' shown in Fig. 6. The results of the comparisons are shown in the three diagrams in Fig. 8, which had values for f_{1c} comparable to the values for f_c' in Fig. 6. The tests by Kani are separately marked and trend lines are given for both datasets.

The tests by Kani in Fig. 8 show, in all cases, the drastic decrease of capacity in the left part of the valley, as in Fig. 6. However, this is not the case for the other tests of the database, which show almost horizontal trend lines. It is only in Fig. 8(c) that the other tests exhibit a slight decrease of capacity with increasing a/d, but this is on a lower level, because the one test for $a/d = 0.78$ did not reach the flexural capacity as assumed for the shear valley. Also, other test series were similarly investigated and yielded similar results, as could be expected from Fig. 7 for all tests.

It can thus be concluded that the tests of the database do not confirm the test results of Kani presented in the left part of the shear valley. This contradicts the theoretical considerations by Kani concerning the arching action, by which he explained the left part of the shear valley. Therefore, in the following the tests are compared with strut-and-tie models, which cover the arching action in the range $\kappa = a/d < 2.4$.

FORCES AND STRESSES OF SIMPLE STRUT-AND-TIE MODEL

Calculation of forces and stresses of model

The forces in the struts and ties of the model in Fig. 1 follow directly from equilibrium and are calculated in the

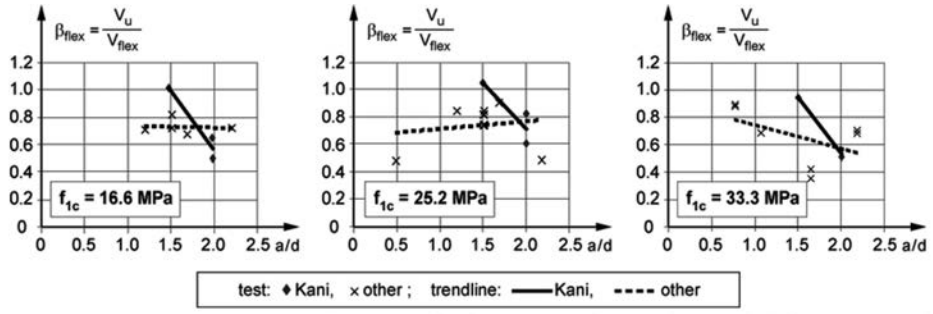

(a) tests with f_{1c} = 2400 psi (3 Kani tests, 5 other) (b) tests with f_{1c} = 3650 psi (3 Kani tests, 10 other) (c) tests with f_{1c} = 4830 psi (3 Kani tests, 7 other)

Fig. 8—Test series by Kani of Fig. 6 compared with other tests of database.

following for beams without axial forces. The tie force F_s is calculated for the maximum moment $M_{max} = F \cdot a$ (refer to Eq. (5a)) and it is constant from midspan to the support

$$F_s = M_{max}/z = F \cdot a/z \quad (7)$$

The maximum compressive force is equal to F_s

$$F_c = F_s = F \cdot a/z \quad (8)$$

The force in the inclined strut is

$$C = F/\sin\theta \quad (9a)$$

$$\text{or at node (N2): } C = F_c/\cos\theta \quad (9b)$$

$$\text{or at node (N1): } C = F_s/\cos\theta \quad (9c)$$

The angle θ follows from the geometry of the model

$$\cot\theta = a/z \quad (10)$$

The area of the strut at the faces of the nodes follow from the geometries shown in Fig. 9, so that the stresses at the ends of the struts can be calculated as follows:

- At node (N1) with $w_t = 2d_1$ and a_A as shown in Fig. 9(a)

$$A_{cs1} = b_w \cdot w_{n1} = b_w \cdot (w_t \cdot \cos\theta + a_A \cdot \sin\theta) \quad (11)$$

$$\sigma_{cn1} = C/A_{cs1} \quad (12)$$

$$\sigma_{cA} = F/(b_w \cdot a_A) \quad (13)$$

- At node (N2); refer to Fig. 9(b)

$$A_{cs2} = b_w \cdot w_{n2} = b_w \cdot (c \cdot \cos\theta + a_F \cdot \sin\theta) \quad (14)$$

$$\sigma_{cn2} = C/A_{cs2} \quad (15)$$

$$\sigma_{cF} = F/(b_w \cdot a_F) \quad (16)$$

$$\sigma_c = F_c/(b_w \cdot c) \quad (17)$$

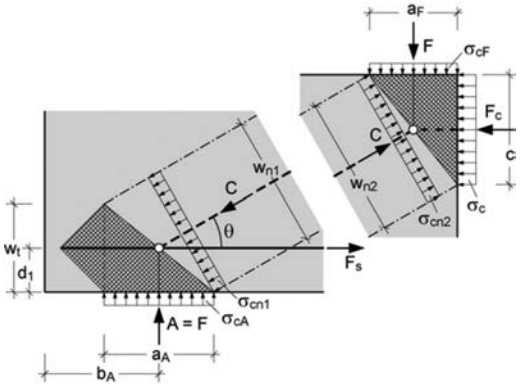

(a) node (N1) (b) node (N2)

Fig. 9—Dimensions and definition of stresses acting on nodes (N1) and (N2).

Strengths of struts, ties, and nodes according to ACI 318-11

Strength of struts—The strength of an unreinforced strut is

$$F_{ns} = A_{cs} \cdot f_{ce} \quad (18)$$

where A_{cs} is the cross-sectional area at one end of the strut; and f_{ce} is the effective compressive strength.

The effective compressive strength is defined as

$$f_{ce} = \beta_s \cdot 0.85 f_c' \quad (19)$$

For unreinforced struts the factor β_s is defined as follows:

- β_s = 1.0 for a strut with uniform cross-sectional area over its length, such as strut F_c in Fig. 1;
- β_s = 0.60 for a strut without reinforcement, such as the inclined strut in Fig. 1.

Strength of ties—The strength of a tie is

$$F_{nt} = A_{ts} \cdot f_{sy} \quad (20)$$

where A_{ts} is the area of nonprestressed reinforcement; and f_{sy} is yield strength.

Strength of nodes—The strength of nodes is defined as

$$F_{nn} = A_{cz} \cdot f_{ce} \quad (21)$$

where A_{cz} is the smaller area of the node face on which F_u acts; and f_{ce} is the effective compressive strength.

The effective compressive strength for nodes is defined as

$$f_{ce} = \beta_n \cdot 0.85 f_c' \quad (22)$$

The factor β_n is $\beta_n = 1.0$ for C-C-C-nodes such as node (N2), and $\beta_n = 0.80$ for C-C-T-nodes such as node (N1).

Procedure for comparisons with tests

When comparing test results with calculated values of a model complying with Appendix A of ACI 318-11, the aforementioned strength values have to be compared with the stresses in the model for the ultimate load of the test beam. Thereby, it must be noted that the term $0.85f_c'$ in the different strength values for the nodes and struts is the design value for the uniaxial compressive strength as defined in RA.3.2. For the tests, this corresponds to f_{1c} derived from the different control specimens for the compressive strength of concrete. Therefore, the following values for the ultimate load F can be derived calculated from the capacities of the members of the strut-and-tie model of Fig. 1.

At the C-C-T-node (N1), the pressure on the support plate is limited to $\beta_s = 0.80$, giving

$$F_1 = 0.80 f_{1c} \cdot a_A \cdot b_w \quad (23)$$

At the C-C-C-node (N2), the pressure on the support plate is limited to $\beta_s = 1.0$, giving

$$F_2 = 1.0 f_{1c} \cdot a_F \cdot b_w \quad (24)$$

The inclined strut acting on node (N1) is limited to $\sigma_{cs1} = 0.60 f_{1c}$, and with Eq. (12), this gives the maximum load F_3

$$F_3 = C_{N1} \cdot \sin\theta = \sigma_{cn1} \cdot A_{cs1} \cdot \sin\theta = 0.60 f_{1c} \cdot A_{cs1} \cdot \sin\theta \quad (25)$$

where, according to Eq. (11), $A_{cs1} = b_w \cdot w_{n1} = b_w \cdot (w_t \cdot \cos\theta + a_A \cdot \sin\theta)$.

At this node (N1), the height of the node should be such that for the vertical face, the limiting stress $0.80 f_{1c}$ is not exceeded, and this gives the following capacity

$$F_4 = 0.80 f_{1c} \cdot b_w \cdot w_t/(a/z) = 0.80 f_{1c} \cdot b_w \cdot w_t/\cot\theta \quad (26)$$

At node (N2), the stress is limited to $\sigma_{cn2} = 1.0 f_{1c}$ at the node face, but decisive is the lower value for the inclined strut of $\sigma_{cs2} = 0.6 f_{1c}$, and this gives the maximum load F_5

$$F_5 = C_{N2} \cdot \sin\theta = \sigma_{cs2} \cdot A_{cs2} \cdot \sin\theta = 0.6 f_{1c} \cdot A_{cs2} \cdot \sin\theta \quad (27)$$

where, according to Eq. (14), $A_{cs2} = b_w \cdot w_{n2} = b_w \cdot (c \cdot \cos\theta + a_F \cdot \sin\theta)$.

From the capacities of the chord forces, the following values can be derived

$$F_6 = F_s/(a/z) = F_s/\cot\theta = A_s \cdot f_{sy}/\cot\theta \quad (28)$$

$$F_7 = F_c/(a/z) = F_c/\cot\theta = 1.0 f_{1c} \cdot b_w \cdot c/\cot\theta \quad (29)$$

where, according to Eq. (10), $\cot\theta = a/z$.

Assuming a stress block in the compression zone, the inner lever arm is

$$z = d - c/2 \quad (30)$$

Dividing this by d gives the following nondimensional values

$$\zeta = 1 - \xi/2 \quad (31)$$

$$\text{where } \xi = c/d \quad (32)$$

It should be noted that Section 11.8.3 of ACI 318-11 is not considered in the following, which specifies the maximum capacity for deep beams.

The solution is determined by the location of the strut force F_c at node (N2) in the distance $c/2$ from the top face. If the depth c of the compression zone is known, the inner lever arm z can be calculated from Eq. (30) and subsequently the strut angle θ from Eq. (10). Then the aforementioned forces can be determined because all the dimensions are given.

For the depth c of the compression zone, assumptions were often made as described by Russo et al. (2005). An often selected value is $c = 0.2d$ corresponding to an inner lever arm of $z = 0.9d$. Sometimes the value for c was derived from the classical bending theory, whereby this is based on a linear stress distribution in the compression zone and not on a stress block usually assumed for strut-and-tie models as shown in Fig. 9(b). Quintero-Febres et al. (2006) and Wight and Parra-Montesinos (2003) assumed a value for c and checked the strut forces in a second trial for it.

In the following, different alternatives for calculating c are presented for the purpose of comparing calculated capacities $F_{u,cal}$ for the simple strut-and-tie model used in Appendix A of ACI 318-11 with test results. The comparison with $F_{u,test} = V_{u,test}$ gives the model safety factor γ_{mod}

$$\gamma_{mod} = F_{u,test}/F_{u,cal} = V_{u,test}/V_{u,cal} \quad (33)$$

This model safety factor characterizes the quality of the model and may be compared with the reverse $1/\phi$ of the strength reduction factor of Section 9.3 of ACI 318-11, respectively, with γ_c in EC 2 or *fib* MC 2010 or FIP Recommendations (1999). It does not contain safety factors for the loads and it is not a global safety factor.

ALTERNATIVES FOR CALCULATING FAILURE LOAD

Alternative 1 for calculated failure load

For calculating the relevant capacity of F_1 to F_7 given by Eq. (23) to (29), an iterative procedure was proposed by Russo et al. (2005) to determine the depth c of the compression zone and the minimum value for the capacity. The condition for the model is that, at node (N2) shown in Fig. 9(b), the stresses σ_{cn2} and σ_c of the inclined strut C_{N2} and the strut F_c simultaneously attain their strength limits. The procedure for the iterations of c starts with the input and an assumed value for c. The value for c is iteratively varied until at the node face of (N2) the inclined strut C_{N2}

is in equilibrium with the inclined resultant of F_c and F. For the final geometry of the model, the minimum value of the capacities F_1 to F_7 is then selected. All calculations and the comparisons with the tests were performed in a spreadsheet.

In almost all cases, the node (N2) was decisive and this is illustrated in Fig. 10 for Beam HB3 by Quintero-Febres et al. (2005, 2006), which has a low slenderness of $a/d = 0.78$. The node height is minimized so that the allowable strengths for the struts F_c and C (also refer to Fig. 1) are attained simultaneously. The result is that this Alternative 1 yields very low values for the depth c of the compression zone and consequently results in high values for the model safety factor, which was $\gamma_{mod} = 1.16$ for Beam HB3 and was, thus, conservative.

Alternative 2 for calculated failure load

It appears to be conclusive that the depth c of the compression zone should not be smaller than that calculated for the flexural capacity at the maximum moment of the beam (refer to Fig. 1), and this is assumed for Alternative 2. Thereby, in the compression zone the stress block of the CEB-FIP MC 90, respectively, of the FIP Recommendations (1999) is assumed, which extends over the complete depth c with a reduced stress of

$$f_{c,eff} = \kappa_c \cdot f_{1c}, \text{ with } \kappa_c = (1 - f_{ck}/250) \quad (34)$$

This method was used for checking the flexural capacity of the tests collected in the shear databases, as explained in detail by Reineck et al. (2006, 2010, 2012).

The depth of the compression zone for the previously discussed Beam HB3 by Quintero-Febres et al. (2005, 2006) is $c = 117$ mm (4.6 in.) or $c/d = 0.307$, and thus far higher than calculated for Alternative 1 with only 47 mm (1.9 in.) or $c/d = 0.125$, as shown in Fig. 10. The consequence is that a higher load is calculated so that the model safety factor γ_{mod} of Eq. (33) is far lower with $\gamma_{mod} = 0.89$ than that of 1.16 for Alternative 1 and is, thus, unconservative.

Alternative 3 for calculated failure load

Because at shear failures the beams do not attain the flexural strength, Alternative 2 may not be appropriate for assessing the depth of the compression zone. Therefore, in the databases for all beams, the depths of the compression zone were also calculated for the load at shear failure, which is lower than the load at the calculated flexural capacity. Thereby, for simplicity, the same assumption was made for the stress-block as above for Alternative 2.

The depth of the compression zone for the previously discussed Beam HB3 by Quintero-Febres et al. (2005, 2006) is, for Alternative 3, $c = 70$ mm (2.7 in.) or $c/d = 0.183$ and is thus lower than that for Alternative 2, but is far higher than for Alternative 1 with only 47 mm (1.9 in.) or $c/d = 0.125$, as shown in Fig. 10. The consequence is that a higher load is calculated so that the model safety factor γ_{mod} of Eq. (33) is lower with $\gamma_{mod} = 1.06$ than that of 1.16 for Alternative 1, but it is on the safe side.

Alternative 4 for calculated failure load

Many shear failures occur at levels far below the flexural capacity so that the stresses in the compression zone are so low that the stress block may not be representative. Therefore, in Alternative 4, the bilinear σ_c-ε_c relationship shown in Fig. 11 was assumed according to Eurocode EC2. The values for the only used elastic range shown in Fig. 11 are defined as follows

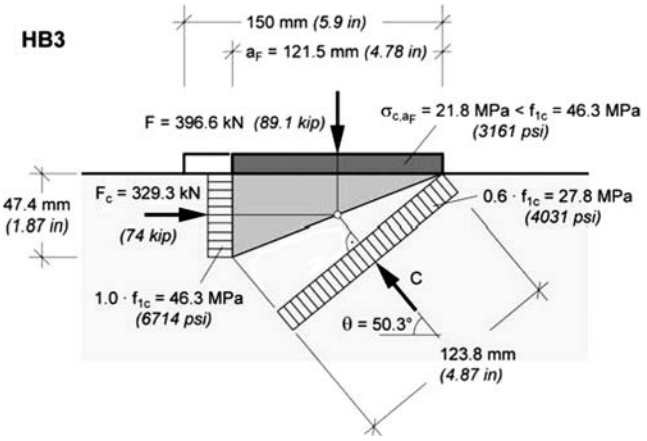

Fig. 10—Dimensions and stresses of node (N2) of Beam HB3 by Quintero-Febres et al. (2005, 2006) calculated for Alternative 1.

$$E_c = f_{1c}/\varepsilon_{c3} \quad \text{elastic modulus of concrete} \quad (35)$$

$$\varepsilon_{c3} = 1.75‰ \text{ if } f_{ck} \le 50 \text{ MPa} \quad (36a)$$

$$\varepsilon_{c3}(‰) = 1.75 + 0.55 \cdot \left(\frac{f_{ck} - 50}{40} \right) \text{ if } f_{ck} > 50 \text{ MPa} \quad (36b)$$

If the compressive stress remains in the linear branch, a simple expression can be given for the depth $\xi = c/d$ of the compression zone of beams without axial forces and without compression reinforcement

$$\xi^2 + 2 \cdot n \cdot \rho \cdot \xi - 2 \cdot n \cdot \rho = 0 \quad (37)$$

where $n = E_s/E_c$ with E_c from Eq. (35); and $\rho = A_s/(b \cdot d)$ = reinforcement ratio.

This relationship (Eq. (37)) was extended by Todisco (2011) to also consider compression reinforcement.

For the linear stress-strain relationship, the inner lever arm is

$$\zeta = 1 - \xi/3 \quad (38)$$

The depth of the compression zone for the previously discussed Beam HB3 by Quintero-Febres et al. (2005, 2006) is $c = 171$ mm (2.7 in.) or $c/d = 0.451$ for Alternative 4 and thus is far higher than for Alternative 1 with only 47 mm (1.9 in.) or $c/d = 0.125$, as shown in Fig. 7, and also higher than for Alternative 2 with $c = 117$ mm (4.6 in.) or $c/d = 0.307$. The consequence is that a higher load is calculated so that the model safety factor γ_{mod} of Eq. (33) is far lower

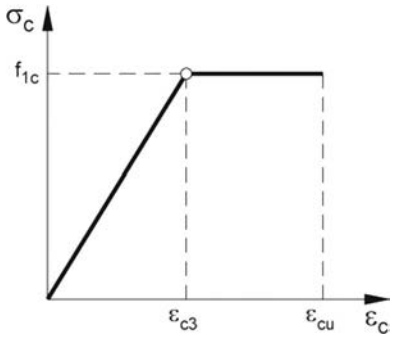

Fig. 11— Bilinear σ_c-ε_c relationship for concrete in compression.

with γ_{mod} = 0.73 than that of 1.16 for Alternative 1 or 0.89 for Alternative 2.

In the calculations, however, it was checked that the elastic range of the compressive stresses (refer to Fig. 11) is not exceeded, and this applied to only 169 tests of all 222. Among these beams was the previously discussed Beam HB3 so that its model safety factor of γ_{mod} = 0.73 is valid.

CONSIDERING THE LIMIT OF APPENDIX A OF ACI 318-11 FOR SIMPLE STRUT-AND-TIE MODEL

The previous calculations showed that the simple model of Fig. 1 appears to be unconservative. However, to come to a final conclusion, the limit of cotθ = a/z = 2.14 of Eq. (1a) according to Appendix A of ACI 318-11 should be considered, and then only 153 tests qualify for the evaluation.

In this dataset, only for 122 tests out of 153 the dimension a_F for the loading plates is given, and therefore in earlier calculations the assumptions $a_F = 0.1h$ was made if this value was not given. This is a rather low value because the average value is $a_F = 0.203h$. To investigate the influence of different assumptions, the calculations for Alternative 3 were repeated for values from $a_F = 0.1h$ to $0.3h$ and the results are given in Table 3. There is a clear trend that, with increasing value for a_F, the number of unsafe tests with $\gamma_{mod} < 1.0$ increases. The assumption of $a_F = 0.1h$ is therefore too favorable for assessing the safety, so that in the following for all Alternatives, the average value $a_F = 0.20h$ is assumed if a_F is not given.

The calculations for the Alternatives 1 to 3 were repeated for only these 153 tests with values $a/z < 2.14$. The results for the statistical values are listed in Table 4 and show that all Alternatives are unconservative.

For Alternative 4, it was checked that the elastic range of the compressive stresses (refer to Fig. 11) was not exceeded, and this applied to only 109 tests of all 153. Therefore, the statistical values for the model safety factor γ_{mod} of Eq. (33) were calculated again for all four Alternatives for these 109 tests and are listed in Table 5. All Alternatives yield unsafe results, and this is especially the case for the more realistic Alternatives 3.3 and 4 with 20% and 40% unsafe tests, respectively.

To make sure not to be dependent on the assumption for the width a_F of the loading plates when finally assessing the safety of the simple model in Fig. 1, the calculation for all Alternatives 1 to 4 were repeated for only the 80 tests out of 109 where the dimension a_F for the loading plate was given. The results of these calculations were very similar to that given in Table 5. All Alternatives yielded unsafe results for the model of Appendix A of ACI 318-11. Thereby, Alternative 3 with approximately 20% unsafe tests and Alternative 4 with even 40% unsafe tests can be regarded as more realistic then Alternatives 1, so that the safety risk is clearly given. This mainly means that the limit of $\beta_s = 0.6$ for an unreinforced strut is not a safe value. If Alternative 3 is used, the value of $\beta_s = 0.6$ for unreinforced struts should be reduced to $\beta_s = 0.415$ to attain only four values with $\gamma_{mod} < 1$ corresponding to the 5% fractile.

For the model of Alternative 3, the model safety factors γ_{mod} are plotted in Fig. 12(a) versus the shear-span ratio $\kappa = a/d$ and shows that the unsafe tests are distributed over the entire range. This reflects that the simple strut-and-tie model of Fig. 1 is only safe for beams without stirrups if the value for the strength of the struts is reduced to approximately β_s = 0.42, as stated previously. For the same tests, the ratios $\beta_{flex} = V_u/V_{flex}$ are plotted versus $\kappa = a/d$ in Fig. 12(b) and these are lower than $\beta_{flex} = 1$ in the entire range. The lowest values occur for low a/d and this clearly complies with the previous finding that the tests of the database do not confirm the left part of the shear valley by Kani in which flexural failures occur for values of $a/d < 1$.

Table 3—Statistical values for γ_{mod}*

Statistical values for γ_{mod}	Alt. 3.1 $a_F = 0.1h$	Alt. 3.2 $a_F = 0.15h$	Alt. 3.3 $a_F = 0.2h$	Alt. 3.4 $a_F = 0.25h$	Alt. 3.5 $a_F = 0.3h$
m	1.435	1.391	1.366	1.350	1.340
s	0.396	0.379	0.380	0.384	0.388
$v = s/m$	0.276	0.272	0.278	0.284	0.289
n with $\gamma_{mod} < 1$	18 = 11.8%	18 = 11.8%	22 = 14.4%	26 = 17.0%	29 = 18.9%

*For Alternatives 3 and with different assumptions for width of loading plates a_F and a_A if not given for the 153 tests with $a/z \le 2.14$.

Table 4—Comparison of statistical values for γ_{mod}*

Statistical values for γ_{mod}	Alt. 1.3	Alt. 2.3	Alt. 3.3
m	1.790	1.332	1.438
s	0.742	0.440	0.380
$v = s/m$	0.414	0.330	0.278
n with $\gamma_{mod} < 1$	15 = 9.8%	34 = 22.2%	22 = 14.4%

*Of the three Alternatives for the 153 tests of the database vuct-RC-A-24 for which slenderness limit of $a/z \le 2.14$ applies.

Table 5—Comparison of statistical values for γ_{mod}*

Statistical values for γ_{mod}	Alt. 1	Alt. 2	Alt. 3.3	Alt. 4
m	1.686	1.195	1.268	1.098
s	0.788	0.377	0.365	0.351
$v = s/m$	0.468	0.315	0.288	0.319
n with $\gamma_{mod} < 1$	15 = 13.8%	34 = 31.2%	22 = 20.2%	44 = 40.4%

*Of the four Alternatives for the 109 tests of the database vuct-RC-A-24 for which the slenderness is $a/z \le 2.14$ and the elastic range of Alternative 4 is valid.

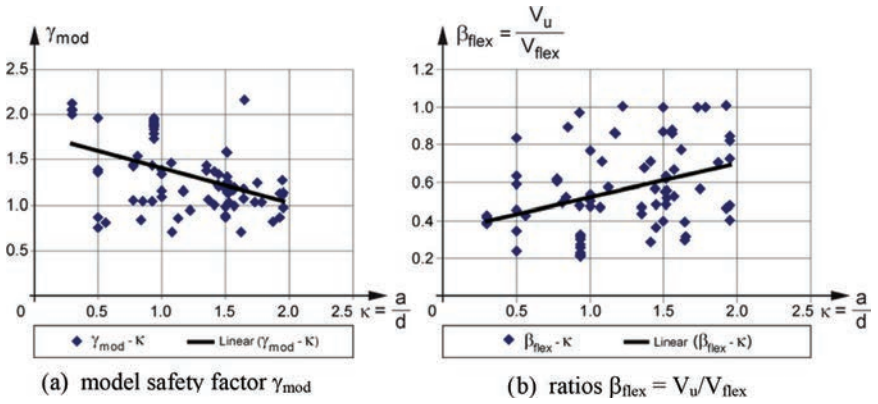

Fig. 12—Model safety factor γ_{mod} and ratios $\beta_{flex} = V_u/V_{flex}$ for Alternative 3 versus shear-span ratio $\kappa = a/d$ for 80 tests with given dimensions a_F for the loading plate.

SUMMARY AND CONCLUSIONS

The database with shear tests on non-slender beams without stirrups subjected to point loads is presented with shear span to effective depth ratios $a/d < 2.4$. The collection database contains 338 shear tests and, after having applied several selection criteria, 222 tests remain for evaluations and comparisons with models or design relationships. The distribution of the number of these tests in selected ranges is presented versus the main parameters for the shear capacity, such as concrete strength, ratio of longitudinal reinforcement, and depths of beams. The overwhelming majority of beams had low concrete strengths of less than 35 MPa (5000 psi) and effective depths $d < 500$ mm (20 in.).

Comparisons were made for beams without stirrups with the left part of the shear valley by Kani according to which the shear capacity increases with decreasing a/d from 2.5 to approximately 1, where the flexural capacity is reached. However, the other tests of the database did not confirm this effect shown by the Kani tests. The reasons for this were further investigated because Kani and others presented theoretical evidence for this. Thereby, strut-and-tie models are appropriate for this range of low slenderness and their capacities were calculated assuming four Alternatives for the depth of the compression zone, which greatly influences the capacity of the model. All alternatives using the strut-and-tie models of Appendix A of ACI 318-11 overestimated the test results. According to the realistic Alternative 3, the value for the strength of the struts should be reduced to approximately $\beta_s = 0.42$ for struts without crossing reinforcement such as in the case of beams without stirrups.

AUTHOR BIOS

Karl-Heinz Reineck, *FACI, is a retired Academic Director of the ILEK (Institute for Lightweight Structures Conceptual and Structural Design) at the University of Stuttgart, Stuttgart, Germany, and Associate Professor of the University of Sarajevo, Bosnia and Herzegovina. He is a member of Joint ACI-ASCE Committee 445, Shear and Torsion.*

ACI member **Leonardo Todisco** *is a Structural Engineer and a PhD Candidate at the Technical University of Madrid, Spain. He received his BS and MS in civil engineering from Technical University of Bari, Bari, Italy, in 2009 and 2011, respectively. His research interests include shear strength of reinforced concrete members and conceptual design of structures.*

ACKNOWLEDGMENTS

The assistance of E. Schnee is greatly acknowledged for improving the drawings.

REFERENCES

ACI Committee 318, 2011, "Building Code Requirements for Structural Concrete (ACI 318-11) and Commentary," American Concrete Institute, Farmington Hills, MI, 503 pp.

EC 2: Eurocode 2, 2004, "Design of Concrete Structures – Part 1: General Rules and Rules for Buildings," EN 1992-1-1. Final draft, Dec.

fib MC, 2010, "*fib* Model Code 2010," final draft, *fib*, Lausanne, Switzerland.

FIP Recommendations, 1999, "Practical Design of Structural Concrete," FIP-Commission 3: Practical Design, Sept. 1996. SETO, London, UK, Sept. (Distributed by: *fib*, http://www.fib-international.org).

Kani, G. N. J., 1964, "The Riddle of Shear Failure and its Solution," *ACI Journal Proceedings*, V. 61, No. 4, Apr., pp. 441-467.

Kani, G. N. J., 1966, "Basic Facts Concerning Shear Failure," *ACI Journal Proceedings*, V. 63, No. 6, June, pp. 675-692.

Quintero-Febres, C.; Parra-Montesinos, G.; and Wight, J. K., 2005, "Evaluation of Strength Factors for Concrete Struts in Deep Concrete Members," *Report* No. UMCEE 05-04, Dept. of Civil and Environmental Engineering, University of Michigan, Ann Arbor, MI, 78 pp.

Quintero-Febres, C. G.; Parra-Montesinos, G.; and Wight, J. K., 2006, "Strength of Struts in Deep Concrete Members Designed Using Strut-and-Tie Method," *ACI Structural Journal*, V. 103, No. 4, July-Aug., pp. 577-586.

Reineck, K.-H.; Kuchma, D. A.; Sim, K. S.; and Marx, S., 2003, "Shear Database for Reinforced Concrete Members without Shear Reinforcement," *ACI Structural Journal*, V. 100, No. 2, Mar.-Apr., pp. 240-249. (discussion, V. 101, No. 1, Jan.-Feb. 2004, pp. 139-144).

Reineck, K.-H.; Kuchma, D. A.; and Fitik, B., 2006, "Erweiterte Datenbanken zur Überprüfung der Querkraftbemessung von Konstruktionsbetonbauteilen ohne und mit Bügel (Extended Databases with Shear Tests on Structural Concrete Beams without and with Stirrups for Assessing Shear Design Procedures)," *Research Report*, ILEK, University of Stuttgart, Stuttgart, Germany. (in German)

Reineck, K.-H.; Kuchma, D. A.; and Fitik, B., 2010, "Extended Databases with Shear Tests on Structural Concrete Beams without and with Stirrups for the Assessment of Shear Design Procedures," *Research Report*, ILEK, University of Stuttgart and University of Illinois-Champaign, Urbana, IL, July.

Reineck, K.-H.; Kuchma, D. A.; and Fitik, B., 2012, "Erweiterte Datenbanken zur Überprüfung der Querkraftbemessung von Konstruktionsbetonbauteilen ohne und mit Bügel (Extended Databases with Shear Tests on Structural Concrete Beams without and with Stirrups for Assessing Shear Design Procedures)," *DAfStb* H. 597, Beuth Verl, Berlin, Germany. (in German)

Reineck, K.-H.; Bentz, E. C.; Fitik, B.; Kuchma, D. A.; and Bayrak, O., 2013, "ACI-DAfStb Database of Shear Tests on Slender Reinforced Concrete Beams without Stirrups," *ACI Structural Journal*, V. 110, No. 5, Sept.-Oct., pp. 867-875.

Russo, G.; Venir, R.; and Pauletta, M., 2005, "Reinforced Concrete Deep Beams—Shear Strength Model and Design Formula," *ACI Structural Journal*, V. 102, No. 3, May-June, pp. 429-437.

Todisco, L., 2011, "Test Evidence for Applying Strut-and-Tie Models to Deep Beams and D-Regions of Beams," master's thesis, Technical University of Bari, Bari, Italy, Oct.

Wight, J. K., and Parra-Montesinos, G., 2003, "Use of Strut-and-Tie Model for Deep Beam Design as Per ACI 318 Code," *Concrete International*, V. 25, No. 5, May, pp. 63-70.